Magnetic Characterization of Soft Magnetic Cores at Cryogenic Temperatures

X. Pei, A. C. Smith, *Senior Member, IEEE,* L. Vandenbossche, and J. Rens

***Abstract*—It is important to investigate and understand the magnetic properties of soft magnetic materials at cryogenic temperatures for the optimal design of superconducting machines and superconducting transformers. The magnetic properties of soft magnetic materials at room temperatures have been studied extensively. However, there is almost no information available for the magnetic properties of these materials at cryogenic temperatures. This paper for the first time presents the experimental results for the magnetic characterization of four soft magnetic materials from room temperature down to 21 K. The experimental results demonstrate that the core losses at 21 K is higher than room temperature for all the materials. They also show that the permeability of all the materials reduce at 21 K compared to room temperature. The optimal temperature in terms of the best magnetic properties is identified for each material. The data presented in this paper will provide valuable guidance for practical design and optimization of superconducting machines and superconducting transformers with soft magnetic cores.**

***Index Terms*—Cryogenics, core loss, magnetic characterization, soft magnetic material, permeability, superconducting machine, superconducting transformer.**

I. Introduction

SUPERCONDUCTING machines offer the significant advantage of higher power density, smaller volume, lighter weight and increased operating efficiencies compared to conventional electrical machines [1]. The applications of superconducting machines include large wind turbine generators [2]-[5], electric aircraft and ship propulsion motors [6]-[8]. Superconducting transformers are also significantly smaller and lighter compared to conventional transformers [9]-[11]. Soft magnetic materials such as electrical steels or nanocrystalline alloys are used to guide the flux and increase power density in superconducting machines and superconducting transformers. The magnetic properties of soft magnetic materials at room temperature have been studied extensively and reported [12]-[14]. However, there is a lack of information on the magnetic properties of these materials at cryogenic temperatures [9]-[11], [15], [16]. The magnetic permeability and losses of electrical steels used in superconducting machines and superconducting transformers are important for efficient design of the devices and choice of operating conditions. An accurate understanding of the behavior of these materials at cryogenic temperatures is crucial in optimizing the design of superconducting machines, superconducting transformers and their cryogenic cooling system.

This paper investigates the magnetic properties of four small ring core samples with different soft magnetic materials from room temperature down to 21 K. In order to compare different core materials, the magnetic properties of one low loss non-oriented electrical steel, one non-oriented steel with enhanced permeability, one grain-oriented electrical steel and one nano-crystalline material were experimentally characterized. These small ring cores were placed into a commercial cryostat, which could be controlled to operate from 20 K to 80 K.

The experimental results demonstrate that that the core losses at 21 K is higher than room temperature for all the materials. The experimental results also show the permeability of all the materials reduced at 21 K compared to room temperature. These four materials however have a different sensitivity to variation in the temperature. The best magnetic properties in terms of permeability and core losses are at different temperatures for these four materials. The paper will include a detailed analysis of the experimental results and the implications for the practical design of superconducting machines and superconducting transformers.

II. Experimental Setup

A. Soft magnetic ring core samples

Four soft magnetic ring cores were prepared by OCAS NV to investigate the effect of different core materials at cryogenic temperatures. Fig. 1 shows four ring core samples before placing into the cryostat. The physical dimension and weight of all four ring cores are summarized in Table I. Sample 1 is a fully-processed, low loss non-oriented (NO) electrical steel. The ring core sample was made of stacked thin lamination layers. Sample 2 is a fully-processed, non-oriented electrical steel with enhanced permeability, which is also laminated. The lamination thickness used in sample 2 was thicker than sample 1. Sample 3 is a grain-oriented (GO) electrical steel ring core which was produced from a stack of thin strips. The thin strips were wound in such a way that the material is always magnetized in its preferred direction. Sample 4 is a Finemet nanocrystalline foil produced by Metglas and was wound radially to form a ring core.

X. Pei is with the Department of Electronic & Electrical Engineering, University of Bath, Bath, BA2 7AY, U.K. (e-mail: x.pei@bath.ac.uk).

A. C. Smith is with the Power and Energy Division, School of Electrical and Electronic Engineering, The University of Manchester, Manchester, M13 9PL, U. K (sandy.smith@manchester.ac.uk).

L. Vandenbossche, and J. Rens are with OCAS N.V., Technologiepark 935, B-9052, Zwijnaarde, Belgium. (lode.vandenbossche@ocas.be, jan.rens@ocas.be).

Fig. 1. Picture of soft magnetic ring core samples: (a) fully-processed, low loss non-oriented steel; (b) fully-processed, non-oriented steel with enhanced permeability; (c) grain-oriented steel; and (d) nano-crystalline alloy Finmet.

TABLE I
DIMENSION OF FOUR RING CORE SAMPLES

Sample	Outer diameter (mm)	Inner diameter (mm)	Height (mm)	Weight (g)
Low loss NO steel	100	86	2	32
NO with enhanced permeability	100	86	2	32
GO steel	90	30	30	1074
Finemet	90	70	20	351

B. *Test circuit*

Fig. 2 shows the schematic diagram of the magnetic measurement test circuit. Each ring core sample is provided with a primary and a secondary winding. The magnetic measurement system consists of a high power linear amplifier to supply current to the primary winding, conditioning electronics, data acquisition system, measurement and control software. All measurements are performed with a sinusoidal flux density waveform in the magnetic circuit. The magnetic field strength in the material is obtained by controlling the primary winding current, whereas the voltage in the secondary winding is constantly measured and integrated to give the value of flux linkage in the magnetic circuit. The current in the primary winding is generated by the high power linear amplifier and controlled through a feedback loop in order to realize a sinusoidal voltage in the secondary winding. The magnetic hysteresis loop in the material is thus directly measured, from which the core losses are derived.

The ring core samples were placed in the cryostat cylindrical test space, which was filled with liquid nitrogen before testing. The cold head of the cryostat was connected to a

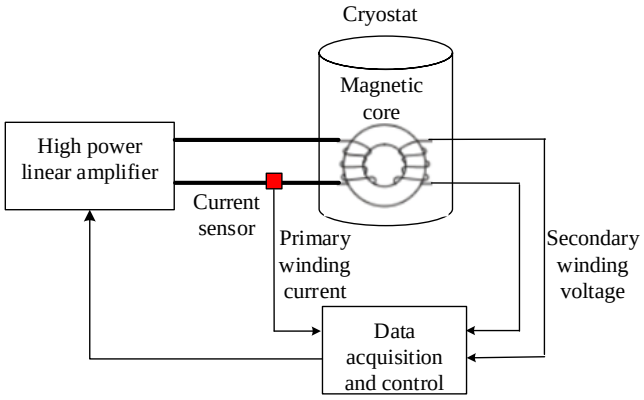

Fig. 2. Schematic diagram of the test circuit.

commercial Cryomech Gifford-McMahon cryocooler [17], [18]. The temperature of the cryostat therefore could be controlled from 20 K to 80 K using the cryocooler and a Lakeshore temperature controller. It should be noted that when the samples were tested below 63 K, the liquid nitrogen in the test space would freeze into solid nitrogen. This did not affect the experimental results as long as the sample cores had a uniform temperature distribution. The temperature of the samples was monitored by a commercial temperature sensor and three calibrated BAS16 diodes. The cryostat has four electrical connections to the cold testing space, which limits the number of cores that can be tested simultaneously to three. The first three materials, low loss non-oriented steel, high permeability non-oriented steel and grain-oriented steel, were tested therefore in the cryostat at identical conditions, whereas the fourth material nano-crystalline alloy Finemet was only measured at two temperatures: liquid nitrogen temperature of 77 K and room temperature.

III. EXPERIMENTAL RESULT AND ANALYSIS

The low loss non-oriented steel, non-oriented steel with enhanced permeability and grain-oriented steel ring core samples were assembled in the cryostat and the cryostat filled with liquid nitrogen. The cryostat was cooled down to 21 K and gradually warmed up in order to characterize the materials at different cryogenic temperatures. The magnetic properties of the low loss non-oriented steel, non-oriented steel with enhanced permeability and grain-oriented steel were measured at 21 K, 42 K, 60 K, 131 K, 180 K, 289 K and 293 K, respectively and over a range of frequencies from 10 Hz to 400 Hz.

Fig. 3 presents the magnetization curve for the low loss non-oriented electrical steel from 21 K to room temperature. The absolute relative permeability of the low loss non-oriented electrical steel is derived from the B-H loop and shown in Fig. 4. As the temperature reduces from room temperature of 293 K, the permeability initially increases as the temperature reduces down to 131 K. When the temperature reduces further from 131 K, the permeability starts to reduce as the temperature reduces. The permeability remains better in the operating temperature range from 42 K to 289 K compared to the per-

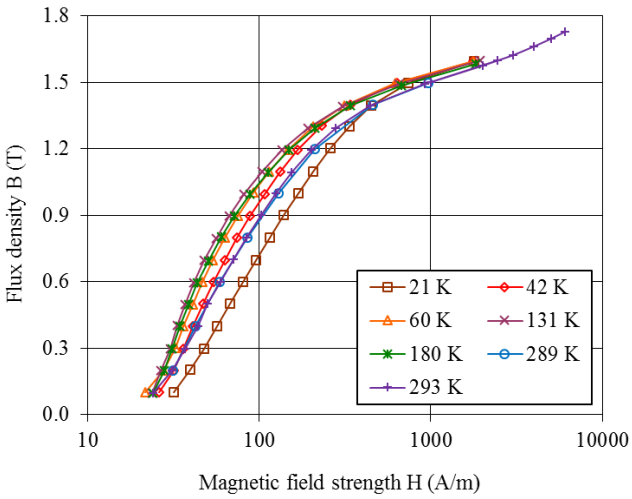

Fig. 3. Magnetization curve of low loss non-oriented steel.

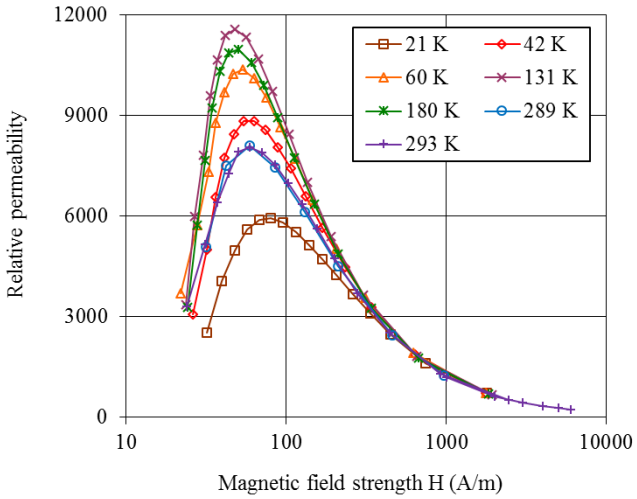

Fig. 4. Relative permeability of low loss non-oriented.

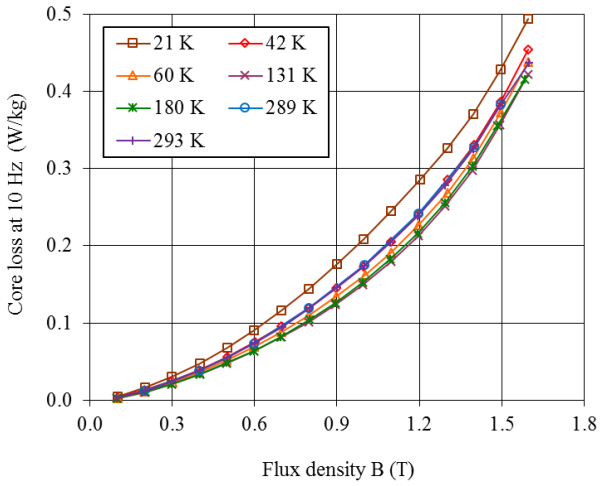

Fig. 5. Core loss of low loss non-oriented steel.

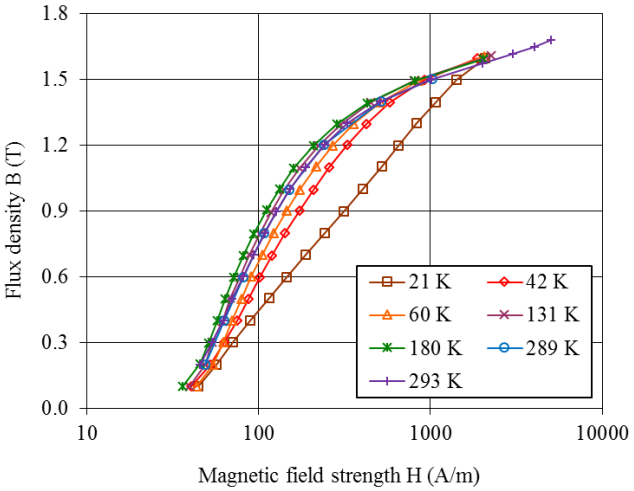

Fig. 6. Magnetization curve of non-oriented steel with enhanced permeability.

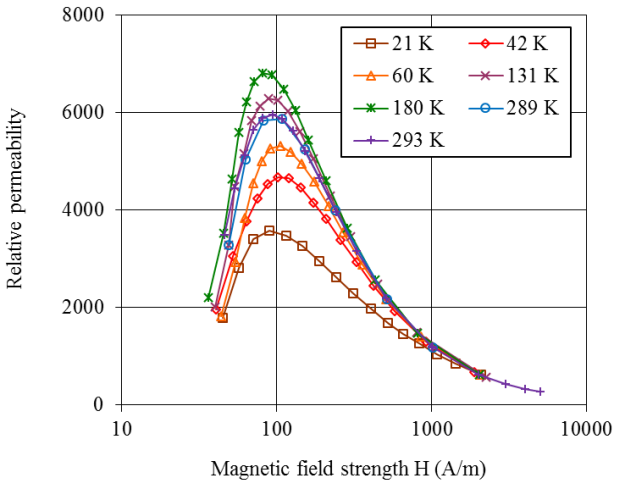

Fig. 7. Relative permeability of non-oriented steel with enhanced permeability.

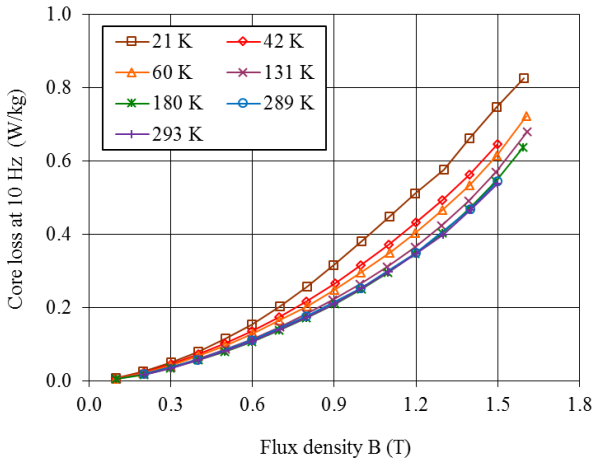

Fig. 8. Core loss of non-oriented steel with enhanced permeability.

meability at room temperature. However, the permeability is lower at 21 K compared to room temperature. The maximum permeability at 131 K is almost twice the maximum permeability at 21 K.

The core losses of the low loss non-oriented electrical steel were measured up to 1.6 T at 10 Hz from 21 K to room temperature and presented in Fig. 5. When the temperature reduces from room temperature to 131 K, the core loss reduces as the temperature reduces. The measured core losses includes

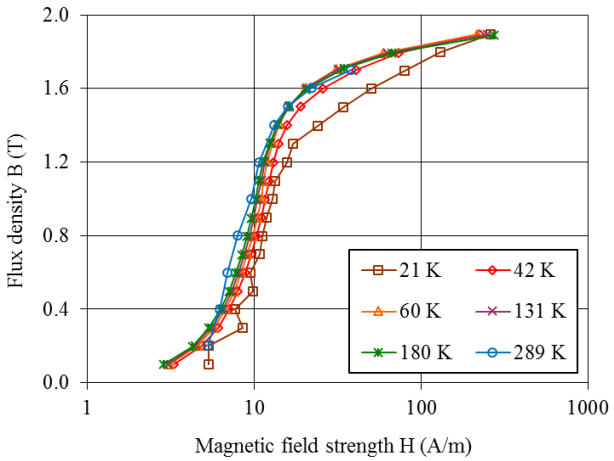

Fig. 9. Magnetization curve of grain-oriented steel.

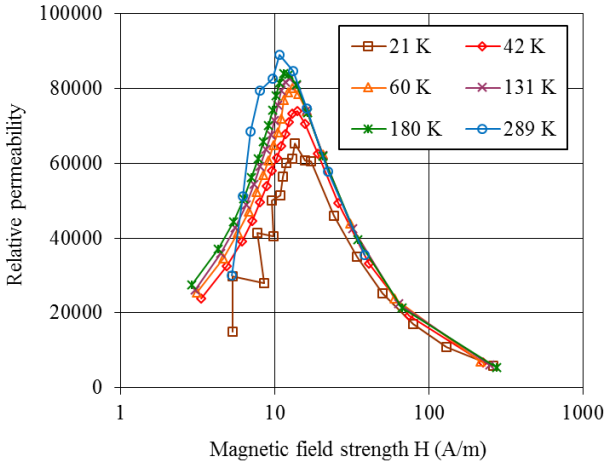

Fig. 10. Relative permeability of grain-oriented steel.

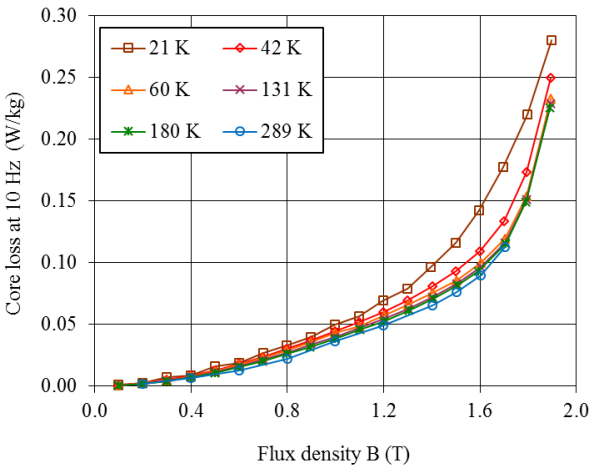

Fig. 11. Core loss of grain-oriented steel.

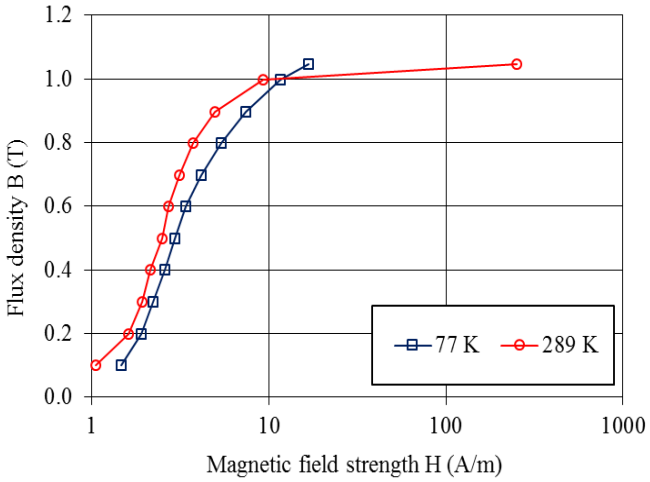

Fig. 12. Magnetization curve of Finemet at 77 K and 289 K.

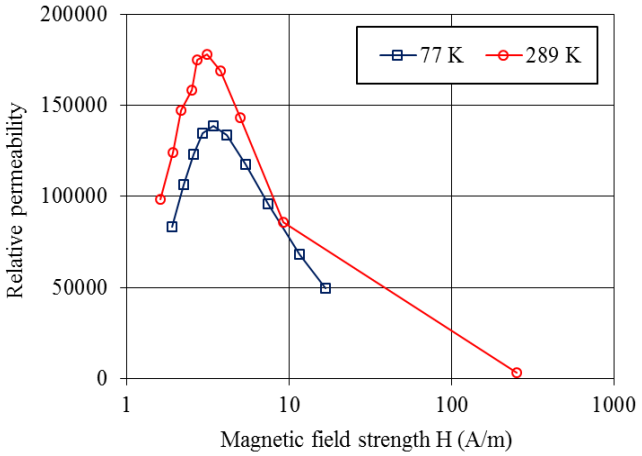

Fig. 13. Relative permeability of Finemet at 77 K and 289 K.

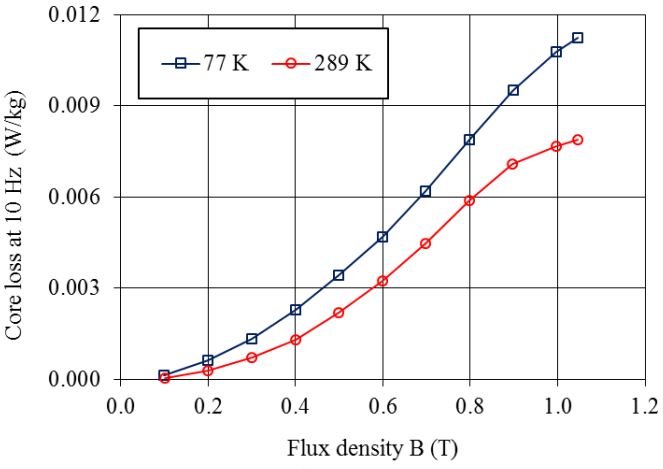

Fig. 14. Core loss of Finemet at 77 K and 289 K.

three classical components of loss (Bertotti model): hysteresis losses, eddy current losses and excess loss [9]-[11]. As the temperature reduces, the electrical conductivity reduces, which results in an increasing eddy current loss and also excess loss. The hysteresis loss however has been shown in previous work to reduce due to the increasing magnetic permeability [10]. The reduction of the core losses from room temperature to 131 K therefore is believed to be caused by the reduction in the hysteresis loss due to the increasing permeability. However, when the temperature reduces below 131 K down to 21 K, the core loss increases as the temperature reduces. As the temperature reduces, eddy current loss and excess loss continues to increase due to the lower electrical conductivity. The hysteresis loss however starts to increase as well due to the reducing magnetic permeability. The core loss at 21 K is approximately 12% higher and the permeability

23% lower than the room temperature values. It is clear that the best magnetic properties for the low loss non-oriented electrical steel with the highest permeability and lowest loss were obtained at 131 K.

Fig. 6 and Fig. 7 show the magnetization curve and relative permeability of the non-oriented steel with enhanced permeability from 21 K to room temperature. The behavior of the non-oriented steel with enhanced permeability is similar to the behavior of the low loss non-oriented electrical steel as both of them are non-oriented electrical steels. This steel was a higher loss steel compared to the first sample so has a larger grain size which reduces the hysteresis loss. The permeability again increases as the temperature reduces to 180 K but the improvement is not as pronounced due to the increased grain size and then starts to reduce as the temperature reduces further. The permeability at 21 K has reduced by 40% from the permeability at room temperature. The maximum permeability at 180 K is almost twice the maximum permeability at 21 K.

Fig. 8 presents the core loss of the non-oriented steel with enhanced permeability up to 1.6 T at 10 Hz from 21 K to room temperature of 289 K. The core loss at the temperature above 180 K is similar to the loss at room temperature. The losses improve marginally as the temperature reduces initially but it is much less pronounced than the low-loss steel probably because the excess loss is more significant in the higher loss steel.

The core loss increases as the temperature reduces below 180 K. The core loss of the non-oriented steel with enhanced permeability at 21 K is approximately 40% higher than the loss at room temperature. The best magnetic properties for the non-oriented steel with enhanced permeability were obtained at 180 K. The higher-loss non-oriented steel with enhanced permeability is not suitable for cryogenic temperature operation due to significant increased core losses. Non-orientated steels are commonly used in electrical machines. At higher frequencies, the trends in the test results were similar for the non-orientated steels but the improved magnetic performance seen at intermediate temperatures, particularly in the first low-loss sample, reduced as the frequency increased due to the increasing eddy current loss component.

Fig. 9 and Fig. 10 present the magnetization curve and relative permeability of grain-oriented from 21 K to 289 K. Grain-orientated steels have larger grain sizes aligned along the magnetization directions and are used in magnetic cores (eg transformers) for example. The magnetization curves at the temperature above 60 K were all similar to the magnetization curve at room temperature so the reducing temperature has less impact on the performance of the grain-orientated steel. The permeability reduces as the temperature reduces below 60 K. Fig. 11 shows the core loss of grain-oriented up to 1.9 T at 10 Hz. The core losses of grain-oriented above 60 K are similar to the loss at room temperature. This indicates that the grain-oriented electric steel could be considered for high temperature superconductor applications above 60 K. The core loss increases when the temperature reduces further from 60 K. The core loss at 21 K is approximately 20% higher than the loss at room temperature. The larger grain size means that the hysteresis loss is reduced and the excess loss increased so the magnetic performance is seen to deteriorate slowly down to 60 K and then more significantly below 60 K.

Fig. 12 to Fig. 14 show magnetization curve, relative permeability and core loss of nano-crystalline alloy Finemet at liquid nitrogen temperature and room temperature. Amorphous steels have no grain structure so this leads to the removal of the excess loss components. They have low hysteresis losses and higher resistivities so produce very low loss materials; however they also have a low saturation density. The nano-crystalline material was also very sensitive to temperature, with a reduction in relative permeability of 20% and an increase in core losses of 40% when the temperature is reduced from room temperature to 77 K.

TABLE II
MAGNETIC PROPERTIES OF FOUR RING CORE SAMPLES

Sample	Temperature of best magnetic properties (K)	Core losses at best temperature/room temperature	Core losses at 21 K/room temperature
Low loss NO steel	131	0.93	1.12
NO steel with enhanced permeability	180	1	1.4
GO steel	289	1	1.2
Finemet	289	1	-

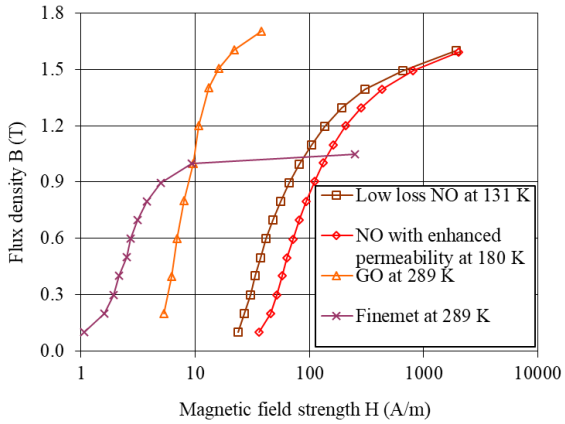

Fig. 15. Magnetization curve of four samples with best magnetic properties.

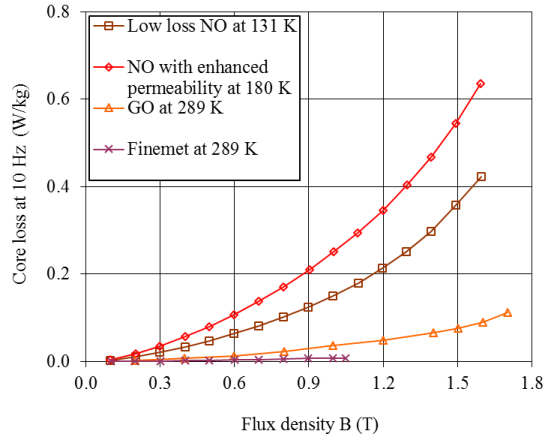

Fig. 16. Core loss of four samples with best magnetic properties.

Table II summarizes the temperature values corresponding to the best magnetic properties and also a core loss comparison for these four samples. It can be noted that the various materials have a different sensitivity to variation in temperature. For example, the magnetic properties of the low loss non-oriented electrical steel vary less from 21 K to room temperature than the non-oriented steel with enhanced permeability. This can be explained by the fact that low loss non-oriented electrical steel has a higher electrical resistivity due to a higher silicon content than non-oriented steel with enhanced permeability, whilst the variation of resistivity with temperature in absolute values is more or less the same for both materials. Therefore, the relative change in resistivity is higher in the non-oriented steel with enhanced permeability, resulting in a greater effect on losses.

Fig. 15 presents the magnetization curve of four samples with best magnetic properties. Finemet has a much higher magnetic permeability and lower saturation flux density than other electric steels. Fig. 16 shows the core loss of four samples with best magnetic properties. The losses in the Finemet core is an order of magnitude lower than the other three materials. The two non-oriented electric steels have higher losses than the grain-oriented steel. The non-oriented steel with enhanced permeability has the worst characteristics in terms of magnetic losses, which is not suitable for cryogenic temperature operation due to significant increased core losses.

In general terms the absolute relative permeability was lower at 21 K than at room temperature for all the materials tested. The permeability of grain-oriented and Finemet samples reduces as the temperature reduces. However, the permeability of the two non-oriented electrical steel are higher at intermediate temperatures between 21 K and room temperature. It was also observed that the core losses are higher at 21 K than at room temperature for all the measured materials and at all frequencies. However, the core losses of the non-oriented electrical steels are lower at intermediate temperatures between 21 K and room temperature.

IV. Conclusion

All four soft magnetic materials investigated in this paper has shown reduced performance in terms of permeability and core losses at 21 K compared to room temperature. The operating temperature to achieve the best magnetic properties has been identified for each soft magnetic material.

These four materials have a different sensitivity to variation in temperature. The magnetic properties of the low loss non-oriented electrical steel grade vary less from room temperature to 21 K than the non-oriented steel with enhanced permeability. The greatest relative change in magnetic properties is observed with the nano-crystalline alloy Finemet material. However, the losses in the Finemet core remain an order of magnitude lower than the other three materials.

References

[1] B. B. Jensen, N. Mijatovic, and A. B. Abrahamsen, "Development of superconducting wind turbine generators," *J. Renew. Sustain. Energy*, vol. 5, no. 2, Mar. 2013, Art. no. 023137.

[2] X. Song *et al*., "A pole pair segment of a 2-MW high-temperature superconducting wind turbine generator," *IEEE Trans. Appl. Supercond*., vol. 27, no. 4, June 2017, Art no. 5201205.

[3] X. Song *et al*., "A full-size high-temperature superconducting coil employed in a wind turbine generator setup," *IEEE Trans. Appl. Supercond*., vol. 27, no. 4, pp. 1-5, Jun. 2017, Art no. 5201105.

[4] R. Qu, Y. Liu, and J. Wang, "Review of superconducting generator topologies for direct-drive wind turbines," *IEEE Trans. Appl. Supercond*., vol. 23, no. 3, Jun. 2013, Art. no. 5201108.

[5] T. Qu *et al*., "Development and testing of a 2.5 kW synchronous generator with a high temperature superconduc ting stator and permanent magnet rotor," *Supercond. Sci. Technol*., vol. 27, 2014, Art. no. 044026.

[6] C. D. Manolopoulos, M. F. Iacchetti, A. C. Smith, K. Berger, M. Husband and P. Miller, "Stator design and performance of superconducting motors for aerospace electric propulsion systems," *IEEE Trans. Appl. Supercond*., vol. 28, no. 4, June 2018, Art no. 5207005.

[7] M. Zhang, F. Eastham and W. Yuan, "Design and modeling of 2G HTS armature winding for electric aircraft propulsion applications," *IEEE Trans. Appl. Supercond*., vol. 26, no. 3, Apr. 2016, Art no. 5205705.

[8] W. Nick, J. Grundmann and J. Frauenhofer, "Test results from Siemens low-speed, high-torque HTS machine and description of further steps towards commercialization of HTS machines," *Physica C*, vol 482, pp. 105-110, 2012.

[9] A. G. Pronto, M. V. Neves, A. L. Rodrigues, "Measurement and separation of magnetic losses at room and cryogenic temperature for three types of steels used in HTS transformers," *J. Supercond. Nov. Magn.*, vol 24, no.1-2, page 981, 2011.

[10] A. G. Pronto, M. V. Neves, A. L. Rodrigues, "A possible solution to reduce magnetic losses in transformer cores working at liquid nitrogen temperature," *Physics Procedia*, vol. 36, pp. 1103-1108, 2012.

[11] A. G. Pronto, A. Maurício and J. M. Pina, "Magnetic properties measurement and discussion of an amorphous power transformer core at room and liquid nitrogen temperature," *J. Phys.: Conf. Ser*, vol. 507, 2014, Art no. 032018.

[12] B. D. Cullity, C. D. Graham, *Introduction to magnetic materials*. Wiley, New Jersey, 2009.

[13] Arnold magnetic technologies. "Soft magnetic applications guide." [Online]. Available: http://www.arnoldmagnetics.com/wp-content/uploads/2017/10/FINAL_Tech-Library_Guides_Soft-Magnetics-Application-Guide.pdf. Accessed on: Jul. 27, 2018.

[14] R. Grössinger, H. Sassik, D. Holzer, N. Pillmayr, "Magnetic characterization of soft magnetic materials-experiments and analysis," *J. Magn. Magn. Mater*., vol 254-255, pp. 7-13, 2003.

[15] P. Song *et al*., "Loss measurement and analysis for the prototype generator with HTS stator and permanent magnet rotor," *Physica C: Superconductivity*, vol. 494, pp. 225-229, 2013.

[16] P. Song *et al*., "Thermal analysis of the HTS stator consisting of HTS armature windings and iron core for a 2.5 kW HTS generator," *Supercond. Sci. Technol*., vol. 29, no. 5, May 2016, Art. no. 054007.

[17] X. Pei, O. Cwikowski, A. C. Smith and M. Barnes, "Design and experimental tests of a superconducting hybrid DC circuit breaker," *IEEE Trans. Appl. Supercond*., vol. 28, no. 3, Apr. 2018, Art no. 5000205.

[18] Cyomech. "Gifford-McMahon cryoreftigerators." [Online]. Available: http://www.cryomech.com/cryorefrigerators/gifford/, Accessed on: Jul. 27, 2018.